Biochimica et Biophysica Acta 1863 (2016) 2175–2188

Contents lists available at ScienceDirect

Biochimica et Biophysica Acta

journal homepage: www.elsevier.com/locate/bbamcr

Integrin-mediated transactivation of P2X7R via hemichannel-dependent ATP release stimulates astrocyte migration

Alvaro Alvarez [a,c,1], Raúl Lagos-Cabré [a,c], Milene Kong [a,c,2], Areli Cárdenas [a,c], Francesca Burgos-Bravo [a,c], Pascal Schneider [d], Andrew F.G. Quest [a,b,c], Lisette Leyton [a,b,c,*]

[a] Cellular Communication Laboratory, Instituto de Ciencias Biomédicas, Facultad de Medicina, Universidad de Chile, 838-0453 Santiago, Chile
[b] Advanced Center for Chronic Diseases, Instituto de Ciencias Biomédicas, Facultad de Medicina, Universidad de Chile, 838-0453 Santiago, Chile
[c] Biomedical Neuroscience Institute, Instituto de Ciencias Biomédicas, Facultad de Medicina, Universidad de Chile, 838-0453 Santiago, Chile
[d] Department of Biochemistry, University of Lausanne, 1066 Epalinges, Switzerland

ARTICLE INFO

Article history:
Received 6 January 2016
Received in revised form 29 April 2016
Accepted 23 May 2016
Available online 25 May 2016

Keywords:
Cell migration
Thy-1
ATP
Calcium
Connexins
Pannexins

ABSTRACT

Our previous reports indicate that ligand-induced $\alpha_V\beta_3$ integrin and Syndecan-4 engagement increases focal adhesion formation and migration of astrocytes. Additionally, ligated integrins trigger ATP release through unknown mechanisms, activating P2X7 receptors (P2X7R), and the uptake of Ca^{2+} to promote cell adhesion. However, whether the activation of P2X7R and ATP release are required for astrocyte migration and whether $\alpha_V\beta_3$ integrin and Syndecan-4 receptors communicate with P2X7R via ATP remains unknown. Here, cells were stimulated with Thy-1, a reported $\alpha_V\beta_3$ integrin and Syndecan-4 ligand. Results obtained indicate that ATP was released by Thy-1 upon integrin engagement and required the participation of phosphatidylinositol-3-kinase (PI3K), phospholipase-C gamma (PLCγ) and inositol trisphosphate (IP3) receptors (IP3R). IP3R activation leads to increased intracellular Ca^{2+}, hemichannel (Connexin-43 and Pannexin-1) opening, and ATP release. Moreover, silencing of the P2X7R or addition of hemichannel blockers precluded Thy-1-induced astrocyte migration. Finally, Thy-1 lacking the integrin-binding site did not stimulate ATP release, whereas Thy-1 mutated in the Syndecan-4-binding domain increased ATP release, albeit to a lesser extent and with delayed kinetics compared to wild-type Thy-1. Thus, hemichannels activated downstream of an $\alpha_V\beta_3$ integrin-PI3K-PLCγ-IP3R pathway are responsible for Thy-1-induced, hemichannel-mediated and Syndecan-4-modulated ATP release that transactivates P2X7Rs to induce Ca^{2+} entry. These findings uncover a hitherto unrecognized role for hemichannels in the regulation of astrocyte migration via P2X7R transactivation induced by integrin-mediated ATP release.

1. Introduction

Integrins are heterodimers of α and β subunits, both of which contain short intracellular domains that lack enzymatic activity and interact with many enzymes, scaffolding proteins, and adaptors to form large protein complexes known as focal adhesions (FAs) [1,2]. FAs are elongated structures that connect the extracellular matrix (ECM) proteins to the cytoskeleton via integrins [3] and thereby mediate cell adhesion to the ECM, an essential event for cell migration [4–6].

Migration is a cyclic process that involves cell polarization, membrane protrusion at the leading edge, FA and stress fiber formation, cell contraction, and retraction of the trailing edge to allow cells to move forward [4,7]. Strong cell adhesion through FAs reduces migration, whereas increased turnover of FAs enhances cell motility. From data available on the composition of the integrin adhesome, a database that has mapped the interactions between 180 or more proteins present in integrin signaling complexes [8,9], it is clear that many receptors and signaling proteins control cell adhesion and migration. One of these proteins is the transmembrane proteoglycan, Syndecan-4, which is involved in promoting anchorage to ECM substrates [10] and binding to other cells [11]. Additionally, in fibroblasts, the binding of Syndecan-4 to fibronectin allows the association of Syndecan-4 with protein kinase C-alpha (PKCα), which activates RhoG and triggers endocytosis of β_1 integrin and increased FA turnover [12]. Thus, Syndecan-4 has been suggested to regulate the transition from strong cell adhesion to cell migration.

Abbreviations: 2-APB, 2-aminoethoxydiphenyl borate; ATP, adenosine 5′-triphosphate; BBG, Brilliant Blue G; EGTA, ethylene glycol tetraacetic acid; ER, endoplasmic reticulum; ECM, extracellular matrix; FAs, focal adhesions; FAK, focal adhesion kinase; FBS, fetal bovine serum; FGF, fibroblast growth factor; HBD, heparin-binding domain; IP3, inositol trisphosphate; IP3R, IP3 receptors; P2X7R, P2X7 receptors; PBS, phosphate-buffer saline; PI3K, phosphatidylinositol-3-kinase; PLCγ, phospholipase-C gamma; PKCα, protein kinase C-alpha; p160ROCK, Rho-associated kinase; s.e.m., standard error of the mean.

* Corresponding author at: Programa de Biología Celular y Molecular, Facultad de Medicina, Universidad de Chile, Santiago, Chile.
E-mail address: lleyton@med.uchile.cl (L. Leyton).
[1] Present address: Faculty of Science, Universidad San Sebastian, Santiago, Chile.
[2] Present address: Department of Biomedicine, Faculty of Health Sciences, University of Antofagasta, Chile.

http://dx.doi.org/10.1016/j.bbamcr.2016.05.018
0167-4889/

Our results indicate that the neuronal glycoprotein Thy-1 interacts with both $\alpha_V\beta_3$ integrin and Syndecan-4 in astrocytes to promote cell adhesion and migration. Ligand-receptor interactions occur through two different domains of the Thy-1 protein: 1) a region containing the arginine-leucine-aspartic acid (RLD) tripeptide, and 2) a heparin-binding domain (HBD), respectively [11,13,14]. Other reports have also confirmed such ligand-receptor binding [15–17]. Thy-1–integrin/Syndecan-4 interactions increase astrocyte adhesion to the ECM [11] and require the recruitment and aggregation of $\alpha_V\beta_3$ integrin. Integrin clustering activates focal adhesion kinase (FAK), Rho-associated kinase (p160ROCK), and RhoA [18]. Integrin signaling also involves PKCα, and possibly inositol trisphosphate (IP3) receptor (IP3R) activation because IP3R inhibitors reduce RhoA activity and astrocyte adhesion induced by Thy-1 [11]. Moreover, prolonged Thy-1 stimulation induces the polarization and migration of DITNC1 astrocytes via the activation of FAK, phosphatidylinositol-3-kinase (PI3K), and the small GTPase Rac1 [19].

Strong astrocyte adhesion induced by Thy-1 also requires increased extracellular adenosine 5′-triphosphate (ATP), activation of the purinergic P2X7 receptor (P2X7R), and Ca^{2+} entry into the cell [20]. Whether this molecular mechanism is also required for cell migration and how ATP is released from the cells to the extracellular media are questions that remain to be explored. Moreover, how these molecular events temporarily connect to the integrin-induced signaling pathways requires further studies.

Under physiological conditions, two general mechanisms for ATP release have been proposed. The first one is exocytic [21,22] and the second one involves the hemichannel proteins [23–30], connexins or pannexins, which are present in astrocytes [31,32]. Connexin hemichannels are well-established gap junction constituents that allow individual cells to communicate with the extracellular medium by permitting the passage of a variety of molecules, such as sugars, small peptides, glutamate, and ATP [33–36]. Pannexins are transmembrane channels that, like connexins, participate in the liberation of ATP and other small molecules through the plasma membrane. Likewise, pannexins also form gap junctions in vitro [29,37,38]. Interestingly, through the release of ATP, hemichannels are known to participate in cell migration events. In fibroblasts, the *C*-terminal domain of Connexin-43 can interact with and modify tubulin and cytoskeletal dynamics [39]. Furthermore, Connexin-43 also impacts on cell polarity [39]. In astrocytes, Connexin-43 is required for cell migration under pro-inflammatory conditions and it interacts with many cytoskeletal proteins, such as β-actin and glial fibrillary acidic protein [40,41]. Conversely, pannexins regulate motility of different cell types, such as neutrophils or leucocytes, tumor cells, venous fibroblasts, and neurons, among others [42–44]. Given these observations, we evaluated whether these hemichannels participate in Thy-1-induced migration of astrocytes by mediating ATP release and P2X7R activation.

Here we show that P2X7R activation is important for cells to migrate in response to Thy-1. Additionally, both Connexin-43 and Pannexin-1 participate in Thy-1-induced ATP release downstream of $\alpha_V\beta_3$ integrin, leading to P2X7R transactivation. We also provide evidence demonstrating that after Thy-1 stimulation, hemichannel opening is modulated by Syndecan-4 and requires PI3K/phospholipase C gamma (PLCγ)-mediated IP3R activation, which leads to the subsequent release of Ca^{2+} from intracellular stores. Together, these findings reveal a novel mechanism linking integrin function to P2X7R transactivation and astrocyte migration via ATP release through hemichannels.

2. Results

2.1. The P2X7 receptor is required for Thy-1-induced astrocyte polarization and migration

We previously demonstrated that the P2X7R is required to increase Ca^{2+} uptake and cell adhesion to the underlying matrix [20]. Here, we set out to study whether P2X7R is also required for Thy-1-stimulated migration of astrocytes. We observed that incubation of DITNC1 astrocytes with the nucleotidase enzyme, Apyrase, precluded Thy-1-induced migration (Fig. 1A), indicating a requirement for ATP. We then tested the effects of different BzATP concentrations (0.1, 1, 5, 10, and 100 μM) on cell migration. BzATP, a non-hydrolyzable ATP analogue, was found to induce cell migration at 10 and 100 μM (control vehicle, 1.0 ± 0.04; [BzATP] = 10 μM, 1.37 ± 0.05, $p < 0.05$; [BzATP] = 100 μM, 1.6 ± 0.1, $p < 0.001$). The latter concentration was used in subsequent experiments (unless indicated otherwise) and coincides with that employed in our previous study [20]. Moreover, migration stimulated by either Thy-1-Fc fusion protein or BzATP was inhibited by two P2X7R antagonists, Brilliant Blue G (BBG) and A438079 (Fig. 1A). The negative control for the Fc-portion of the Thy-1 fusion proteins used in these experiments (Trail-R2-Fc; see Methods) behaved similarly to the control with serum-free medium (Fig. 1A).

To confirm the role of the P2X7R in wound closure, cell migration was evaluated following knockdown of this receptor. Importantly, the siRNA for P2X7R used in these experiments decreases P2X7R mRNA levels without affecting the mRNA levels of other P2X receptors [20]. Here, we demonstrate that diminished P2X7R protein levels (Fig. 1B, insert) blocked migration of astrocytes induced by Thy-1-Fc but had no effect on Trail-R2-Fc-treated cells (Fig. 1B).

The role of P2X7R was also tested in a cell polarization assay. Reorientation of the Golgi apparatus towards the leading edge was evaluated as previously described [19,45]. The increased number of polarized DITNC1 cells induced by either Thy-1-Fc or BzATP was reduced by BBG and A438079 (Fig. 1C). Therefore, P2X7R-mediated events required for astrocyte adhesion to the underlying matrix [20] are also essential for cell polarization and migration induced by Thy-1.

2.2. Thy-1 induces ATP release and cell migration dependent on integrin and Syndecan-4 engagement

To investigate the mechanism involved in ATP release upon Thy-1 addition, extracellular ATP was measured at different time points following the stimulation of astrocytes with various previously described Thy-1 mutants [11,13]. First, SDS-PAGE and Coomassie Blue staining were employed to assess the quality of the Thy-1 mutants. The results revealed the presence of a single band in all cases (Fig. 2A). In addition, Thy-1-Fc induced astrocyte migration, whereas neither the single-domain Thy-1 mutated molecules [Thy-1(RLE)-Fc or Thy-1(AEAAA)-Fc] nor the double mutant [Thy-1(RLE/AEAAA)-Fc] induced astrocyte migration [19] (Fig. 2A, bottom panel). Moreover, to demonstrate the functionality of different Thy-1 proteins, single-domain mutants were combined and migration was then evaluated. When both mutant proteins were added in combination, the increase in migration observed was similar to the effect obtained with the wild-type Thy-1-Fc molecule (Fig. 2A, bottom panel), indicating that the individual mutations did not disrupt the Thy-1 structure.

Subsequently, ATP levels were measured upon treating astrocytes with each of the four different Thy-1 molecules. Thy-1 mutated in the HBD [Thy-1(AEAAA)-Fc] (Fig. 2B, squares) led to a delayed release of less ATP compared to non-mutated Thy-1-Fc protein (Thy-1-(RLD)-Fc; Fig. 2B, circles). Upon stimulation of astrocytes with Thy-1 mutated in the integrin-binding domain [Thy-1(RLE)-Fc], which possesses an intact HBD that permits binding to Syndecan-4, no changes in extracellular ATP levels were observed (Fig. 2B upright triangles). In addition, Thy-1 mutated in both binding sites [Thy-1(RLE/AEAAA)-Fc] did not result in ATP release (Fig. 2B, inverted triangles). These findings, together with results indicating that BzATP added at concentrations >10 μM suffice to induce cell migration (Fig. 1A), led us to hypothesize that the molecular changes leading to ATP release in Thy-1-stimulated DITNC1 cells are triggered by $\alpha_V\beta_3$ integrin engagement, whereas signaling pathways downstream of Syndecan-4 do not trigger ATP release, but rather appear necessary to modulate integrin-induced ATP release. To test this hypothesis, cells were treated with BzATP at

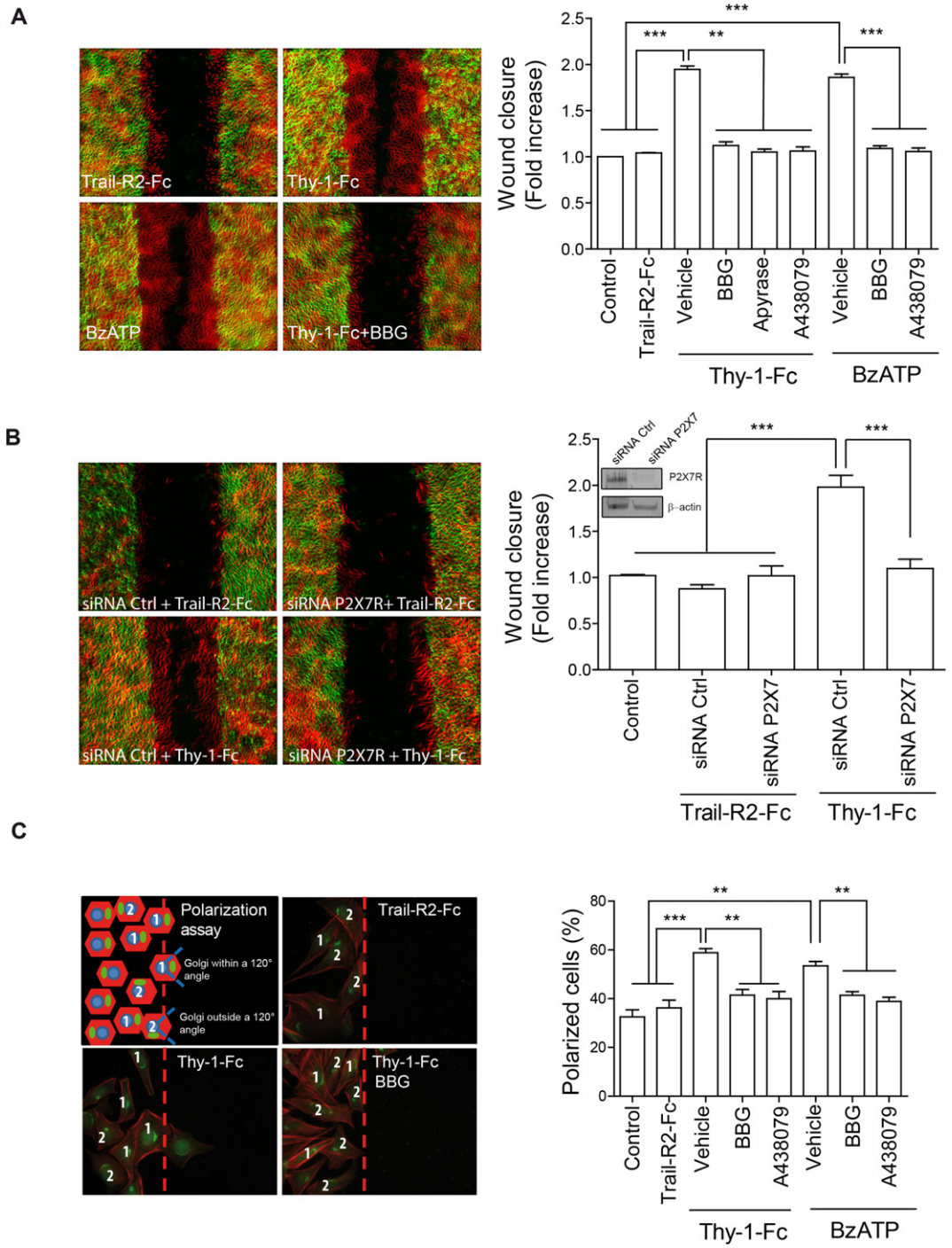

Fig. 1. ATP-activated P2X7 receptor is required for Thy-1-induced astrocyte migration and polarization. Wounded monolayers of cells were treated as indicated below in serum-free medium. A) Representative microphotographs of cells migrating in a wound-healing assay are shown. Cells in a wounded monolayer at time 0 and 24 h are shown in green and red, respectively (virtual colors). The graph shows the quantitative analysis of cell migration after 24 h. Non-treated DITNC1 astrocytes (control) or astrocytes previously treated with vehicle (phosphate-buffer saline; PBS), BBG (5 μM), Apyrase (3 U/ml) or A438079 (100 nM). Where indicated, astrocytes were treated with Trail-R2-Fc (negative control), Thy-1-Fc or BzATP (100 μM) for 24 h. Values of wound closure were obtained by estimating the cell-free area at 0 and 24 h. Wound closure (fold-increase) was calculated as a ratio of the values obtained for every sample divided by those obtained for the non-stimulated samples (control in serum-free medium). Values are expressed as means ± s.e.m. B) Cells transfected with siRNA against P2X7R or a control siRNA were stimulated with the indicated treatments, and wound closure was determined and shown as indicated in A. Insert in the graph shows decreased P2X7R protein levels upon appropriate siRNA treatment. C) Cell polarization assay of DITNC1 astrocytes treated with vehicle, BBG, or A438079 and then treated with Trail-R2-Fc, Thy-1-Fc, or BzATP for 7 h. Schematic representation of polarized cells (top left panel) with Golgi (green) oriented within a 120° angle (blue dashed lines) towards the wounded area (right of the red dashed line) and positioned in front of the nucleus (blue). Representative microphotographs of polarized (marked as 1) and non-polarized (marked as 2) cells with the different treatments are shown. Values in the graph represent means ± s.e.m. of the quantifications obtained as the percentage of polarized cells. Only the first two rows of cells at the wound border were counted. **, $p < 0.01$; ***, $p < 0.001$, evaluated from three independent experiments.

suboptimal concentrations (<10 μM) in conjunction with either Thy-1(RLE)-Fc or Thy-1(AEAAA)-Fc. Neither BzATP added at 0.1 or 1 μM nor the mutants added individually stimulated cell migration (Fig. 2B, C). Moreover, low BzATP concentrations, added with Thy-1-Fc, which binds integrin only [Thy-1(AEAAA)-Fc], did not affect cell migration (Fig. 2C). However, BzATP added simultaneously with mutated Thy-1-Fc, which only binds through the HBD [Thy-1(RLE)-Fc], induced cell migration (Fig. 2D).

To provide direct evidence for the participation of $\alpha_V\beta_3$ integrin, and Syndecan-4 as Thy-1 receptors involved in ATP release, we then silenced either β_3 integrin, or Syndecan-4 and measured ATP release upon Thy-1 addition. Non-transfected cells or cells transfected with scramble siRNA increased extracellular levels of ATP when stimulated with Thy-1 (Fig. 2E). The extent of ATP release did not change significantly in cells stimulated following transfection with integrin- or Syndecan-4-targeting siRNA (Fig. 2E). Importantly, these results were similar to those obtained with Thy-1 mutated in the HBD (Fig. 2B). Altogether, the results indicate that Thy-1 binding to $\alpha_V\beta_3$ integrin

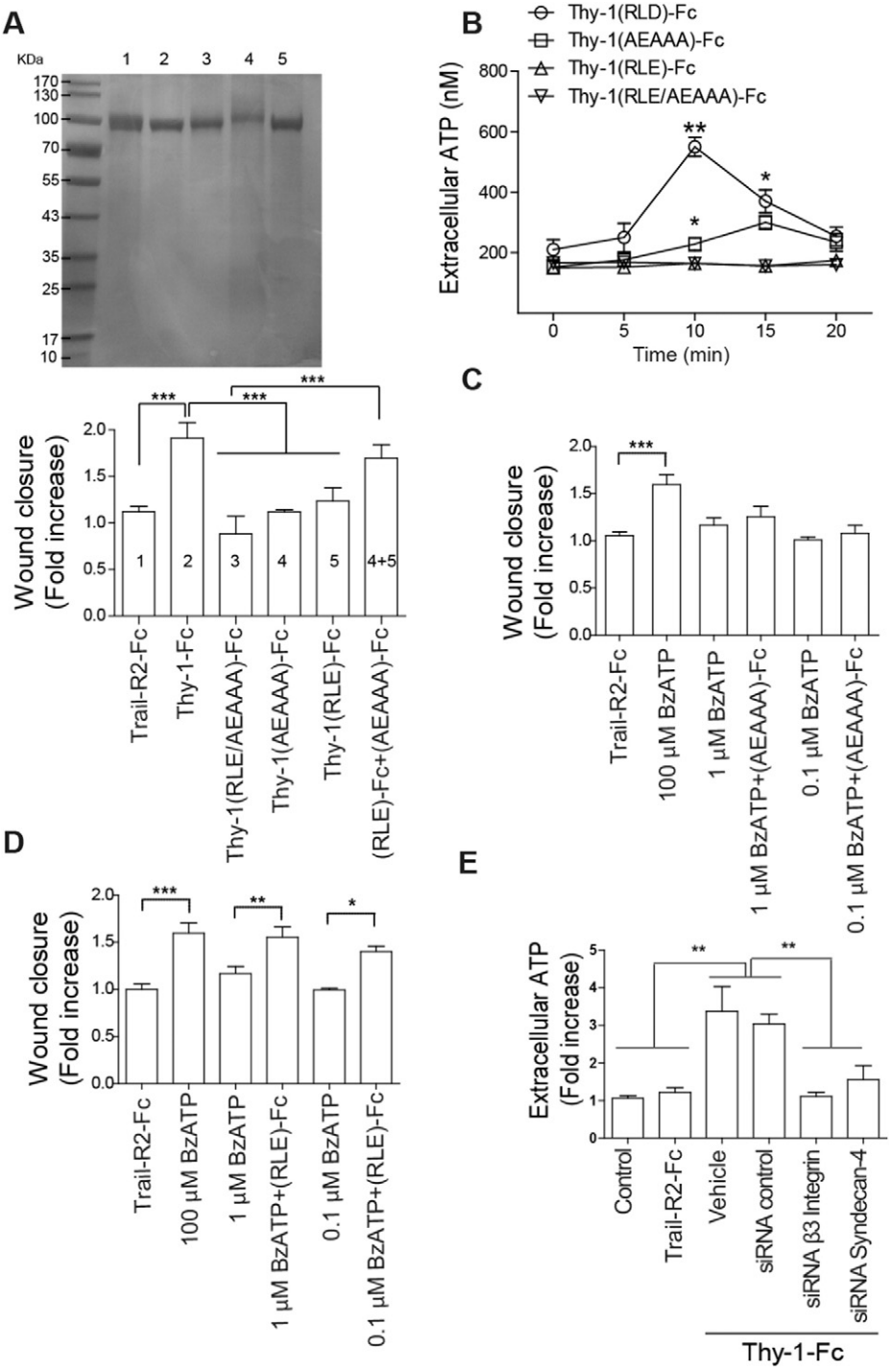

Fig. 2. Thy-1 induces ATP release and wound closure in an integrin-dependent manner. A) Quantitative analysis of DITNC1 astrocyte migration upon treatment with the different Thy-1-Fc mutants for 24 h. Bands in the gel correspond to the 5 different Fc fusion proteins used in this study: (1) Trail-R2-Fc, (2) Thy-1-Fc, (3) Thy-1(RLE/AEAAA)-Fc, (4) Thy-1(AEAAA)-Fc and (5) Thy-1(RLE)-Fc. Wound closure was estimated upon treatment with these Fc proteins as indicated in figure 1A. (RLE)+(AEAAA)-Fc (4+5) indicates cells treated with both mutated Thy-1 proteins together. B) DITNC1 astrocytes were stimulated with the different Thy-1-Fc mutants and at the indicated time points ATP was measured in supernatants. Values in the graph represent means ± s.e.m. from four independent experiments. C-D) Wound closure assay of cells stimulated simultaneously with 0.1 or 1 µM of BzATP and Thy-1(AEAAA)-Fc (C) or Thy-1(RLE)-Fc (D) for 24 h. BzATP (100 µM) was used as a positive control. E) Integrin subunit β3 or Syndecan-4 were silenced by transfection of DITNC1 cells with siRNA targeting these receptors. Cells transfected with a scrambled siRNA provided by the manufacturer were used (see Methods section) as a control. After 48 h of recovery and 30 min in serum-free medium containing nuclease inhibitor, cells were stimulated with Thy-1-Fc (or TRAIL-R2-Fc as negative control) and ATP release was evaluated. *, $p < 0.05$; **, $p < 0.01$; ***, $p < 0.001$ calculated from three independent experiments. Error bars are s.e.m.

leads to ATP release, but that optimal levels are attained following the interaction of Thy-1 with both receptors. This suggests that Syndecan-4 engagement provides a positive feedback loop necessary to reach threshold ATP levels required for astrocyte migration.

A) Quantitative analysis of DITNC1 astrocyte migration upon treatment with the different Thy-1-Fc mutants for 24 h. Bands in the gel correspond to the 5 different Fc fusion proteins used in this study: (1) Trail-R2-Fc, (2) Thy-1-Fc, (3) Thy-1(RLE/AEAAA)-Fc, (4) Thy-1(AEAAA)-Fc and (5) Thy-1(RLE)-Fc. Wound closure was estimated upon treatment with these Fc proteins as indicated in Fig. 1A. (RLE) + (AEAAA)-Fc (4 + 5) indicates cells treated with both mutated Thy-1 proteins together. B) DITNC1 astrocytes were stimulated with the

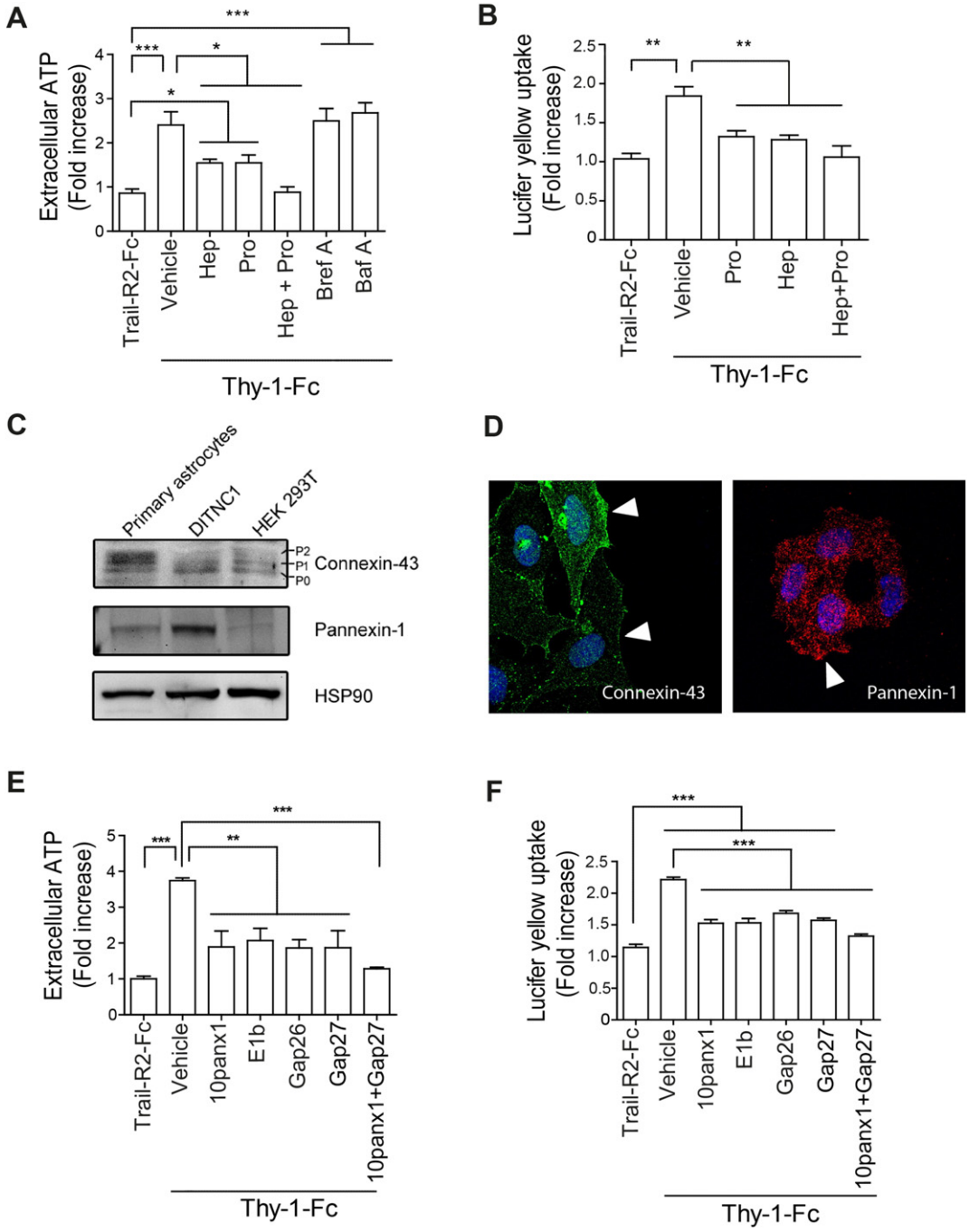

Fig. 3. Thy-1 induces ATP release through Connexin-43 and Pannexin-1 hemichannels. A) ATP values after 10 min of Thy-1 addition were determined in the supernatants of cultured cells previously incubated for either 30 min with Heptanol (500 μM), Probenecid (1 mM), or a combination of both inhibitors, or 4 h with the exocytosis inhibitors, Brefeldine A (3 μg/ml) or Bafilomycin A (1 μM). Cells were then treated with Thy-1 or Trail-R2-Fc (negative control). B) Lucifer Yellow uptake in DITNC1 cells treated with Trail-R2-Fc, stimulated with Thy-1-Fc for 10 min, or treated with the indicated inhibitors for 30 min prior to Thy-1 addition. Values in the graph are mean fluorescence intensity normalized to the non-stimulated condition. C) Cell lysates of DITNC1 cells, primary astrocytes, and HEK293T cells were immunoblotted for Connexin-43, Pannexin-1, and HSP90 as a loading control. Proteins are indicated to the right of the panels. P0, P1 and P2 correspond to multiple electrophoretic forms of the Connexin-43 [51]. D) DITNC1 cells were fixed and permeabilized prior to staining. Hemichannel presence was evaluated by immunofluorescence using anti-Connexin-43 and anti-Pannexin-1 antibodies followed by the corresponding secondary antibodies (green and red, respectively). Nuclei were stained with DAPI (blue). E) Extracellular ATP levels in cells treated with Trail-R2-Fc or Thy-1-Fc for 10 min after treating with vehicle (0.001% DMSO/PBS); the Pannexin-1-blocking peptides, 10panx1 (100 μM) and E1b (100 μM); the Connexin-43-blocking peptides, Gap26 (300 μM) and Gap27 (300 μM); or a mixture of 10panx1 and Gap27 for 30 min. F) Lucifer Yellow uptake in cells stimulated with Trail-R2-Fc or Thy-1-Fc for 10 min and previously treated with the indicated hemichannel-blocking peptides for 30 min. Values shown in all graphs are the means ± s.e.m. from four independent experiments. *, $p < 0.05$; **, $p < 0.01$; ***, $p < 0.001$.

different Thy-1-Fc mutants and at the indicated time points ATP was measured in supernatants. Values in the graph represent means ± s.e.m. from four independent experiments. C-D) Wound closure assay of cells stimulated simultaneously with 0.1 or 1 μM of BzATP and Thy-1(AEAAA)-Fc (C) or Thy-1(RLE)-Fc (D) for 24 h. BzATP (100 μM) was used as a positive control. E) Integrin subunit β3 or Syndecan-4 was silenced by transfection of DITNC1 cells with siRNA targeting these receptors. Cells transfected with a scrambled siRNA provided by the manufacturer were used (see Methods section) as a control. After 48 h of recovery and 30 min in serum-free medium containing nuclease inhibitor, cells were stimulated with Thy-1-Fc (or TRAIL-R2-Fc as negative control) and ATP release was evaluated. *, $p < 0.05$; **, $p < 0.01$; ***, $p < 0.001$ calculated from three independent experiments. Error bars are s.e.m.

2.3. Thy-1 induces ATP release through Connexin-43 and Pannexin-1 hemichannels

To gain further insight into the mechanism of ATP release, extracellular ATP was monitored after stimulating the astrocytes with Thy-1 in the presence or absence of two Golgi-perturbing agents, Bafilomycin A and Brefeldin A [46]. These agents did not affect Thy-1-induced ATP release, indicating that exocytosis is not relevant for this process (Fig. 3A).

ATP release to the extracellular space in response to various stimuli also occurs through connexin/pannexin hemichannels [31]. To assess whether these hemichannels participate in Thy-1-induced ATP release, several hemichannel blockers were tested. The pannexin inhibitor, Probenecid, and the connexin inhibitor, Heptanol, decreased extracellular ATP levels individually, but residual levels were still higher than those observed in the negative controls. However, a combination of both inhibitors reduced ATP levels to those observed in controls (Fig. 3A). To obtain direct evidence for hemichannel opening, we performed a dye uptake assay using the low molecular weight fluorescent dye, Lucifer Yellow, a membrane impermeable molecule that can only be taken up by cells upon the opening of hemichannels [31,47]. As expected, Thy-1-induced Lucifer Yellow uptake was inhibited by Probenecid and Heptanol as well as a combination of both inhibitors (Fig. 3B).

The principal hemichannels in astrocytes are Pannexin-1 and Connexin-43 [48,49]. Therefore, the existence of these proteins in DITNC1 cells was first confirmed by Western blot analysis (Fig. 3C). The bands observed are similar to those detected in primary astrocytes and the human embryonic kidney 293T cells used as controls (Fig. 3C). Immunofluorescence assays performed on cells at low confluency revealed that both Connexin-43 and Pannexin-1 were detectable at non-junctional cell borders, indicative of a hemichannel configuration (Fig. 3D). We then confirmed the results by using more specific astrocyte hemichannel blockers. Pannexin-1 was blocked with the peptides, 10panx1 and E1b [31,47,50], which recognize the extracellular loop domain of Pannexin-1, while Connexin-43 was inhibited with the blocking peptides, Gap26 and Gap27 [31,47]. When used individually, these peptides partially repressed the increase in extracellular ATP (Fig. 3E) and Lucifer Yellow uptake (Fig. 3F) stimulated by Thy-1. However, as observed previously with Probenecid and Heptanol, the combination of both connexin- and pannexin-blocking peptides completely abolished Thy-1-induced ATP release (Fig. 3E) as well as dye uptake (Fig. 3F).

A) ATP values after 10 min of Thy-1 addition were determined in the supernatants of cultured cells previously incubated for either 30 min with Heptanol (500 μM), Probenecid (1 mM), or a combination of both inhibitors, or 4 h with the exocytosis inhibitors, Brefeldine A (3 μg/ml) or Bafilomycin A (1 μM). Cells were then treated with Thy-1 or Trail-R2-Fc (negative control). B) Lucifer Yellow uptake in DITNC1 cells treated with Trail-R2-Fc, stimulated with Thy-1-Fc for 10 min, or treated with the indicated inhibitors for 30 min prior to Thy-1 addition. Values in the graph are mean fluorescence intensity normalized to the non-stimulated condition. C) Cell lysates of DITNC1 cells, primary astrocytes, and HEK293T cells were immunoblotted for Connexin-43, Pannexin-1, and HSP90 as a loading control. Proteins are indicated to the right of the panels. P0, P1 and P2 correspond to multiple electrophoretic forms of the Connexin-43 [51]. D) DITNC1 cells were fixed and permeabilized prior to staining. Hemichannel presence was evaluated by immunofluorescence using anti-Connexin-43 and anti-Pannexin-1 antibodies followed by the corresponding secondary antibodies (green and red, respectively). Nuclei were stained with DAPI (blue). E) Extracellular ATP levels in cells treated with Trail-R2-Fc or Thy-1-Fc for 10 min after treating with vehicle (0.001% DMSO/PBS); the Pannexin-1-blocking peptides, 10panx1 (100 μM) and E1b (100 μM); the Connexin-43-blocking peptides, Gap26 (300 μM) and Gap27 (300 μM); or a mixture of 10panx1 and Gap27 for 30 min. F) Lucifer Yellow uptake in cells stimulated with Trail-R2-Fc or Thy-1-Fc for 10 min and previously treated with the indicated hemichannel-blocking peptides for 30 min. Values shown in all graphs are the means ± s.e.m. from four independent experiments. *, $p < 0.05$; **, $p < 0.01$; ***, $p < 0.001$.

2.4. Thy-1-induced ATP release through hemichannels requires intracellular calcium release through IP3 receptor channels

Our results suggest that, upon Thy-1 stimulation, integrin-dependent signaling pathways lead to ATP release via both types of hemichannels (Fig. 3) and that Ca^{2+} influx depends on the activation of the P2X7R [20]. Thus, we expected hemichannel blockers to inhibit intracellular Ca^{2+} increase. To evaluate this possibility, Ca^{2+} levels were tested in cells following Thy-1 stimulation in the presence or absence of the hemichannel blockers. Probenecid and Heptanol as well as a combination of both partially reduced Thy-1-induced $[Ca^{2+}]_i$ increase after 5 min of stimulation (Fig. 4A), suggesting that Ca^{2+} increase is not only attributable to extracellular influx, but that it also depends on Ca^{2+} release from intracellular stores.

Because ATP release induced by Thy-1 was efficiently blocked by the presence of Probenecid/Heptanol (Fig. 3A), the possibility that the remaining Ca^{2+} signal stems from P2X7R activation seemed rather unlikely. To identify other possible Ca^{2+} sources, different strategies were employed. As expected, when Ca^{2+}-free medium supplemented with ethylene glycol tetraacetic acid (EGTA, a Ca^{2+} chelator) was employed, residual levels of intracellular Ca^{2+} were similar to those described above (Fig. 4B, blue triangles, compare to Fig. 4A, red diamonds). Alternatively, chelation of intracellular Ca^{2+} with the cell permeable BAPTA-acetoxymethyl ester (BAPTA-AM) reduced $[Ca^{2+}]_i$ to non-stimulated levels (Fig. 4B). Importantly, the IP3R inhibitors, 2-aminoethoxydiphenyl borate (2-APB) and Xestospongine B (Xestosp B), almost completely eliminated intracellular Ca^{2+} levels (Fig. 4C), whereas Ryanodine did not alter Thy-1-stimulated Ca^{2+} increases (Fig. 4C) when used at concentrations known to inhibit the intracellular Ryanodine receptor Ca^{2+} channel [52]. These results indicate that, following Thy-1 stimulation, intracellular Ca^{2+} levels are regulated by both influx from the extracellular medium and release from intracellular stores. In addition, intracellular Ca^{2+} release requires IP3R but not Ryanodine receptor activation.

To confirm the importance of this Thy-1-induced Ca^{2+} release, additional Lucifer Yellow uptake and ATP release assays were performed in the presence of the different inhibitors described above. As for the Ca^{2+} signal, BAPTA-AM, 2-APB, and Xestospongine B prevented Lucifer Yellow uptake (Fig. 4D) and ATP release (Fig. 4E), whereas this was not the case in the presence of Ryanodine or Ca^{2+}-free medium (Fig. 4D, E). Lucifer Yellow uptake occurs in medium lacking calcium because this condition opens hemichannels [21,53], and accordingly, ATP release was observed in Ca^{2+}-free medium (Fig. 4E). To test whether Xestospongine B directly modulated hemichannels, the effect of this IP3R inhibitor was tested in Ca^{2+}-free medium. We found that hemichannels opened in medium without Ca^{2+} even in the presence of Xestospongine B (Fig. 4F), demonstrating that Xestospongine-mediated inhibition was specific for IP3R-dependent Ca^{2+} release and did not affect hemichannel function per se. Therefore, we then tested whether the source of IP3 that activated the IP3R was due to

PLCγ activation. As expected, U73122-mediated PLCγ inhibition precluded ATP release induced by Thy-1-Fc in DITNC1 astrocytes (Fig. 4G). Additionally, given that LY294002-mediated inhibition of PI3K also reduced ATP release (Fig. 4G), we reasoned that ATP release requires PI3K activation. Taken together, these observations suggest that Thy-1 induces PLCγ- and PI3K-dependent release of

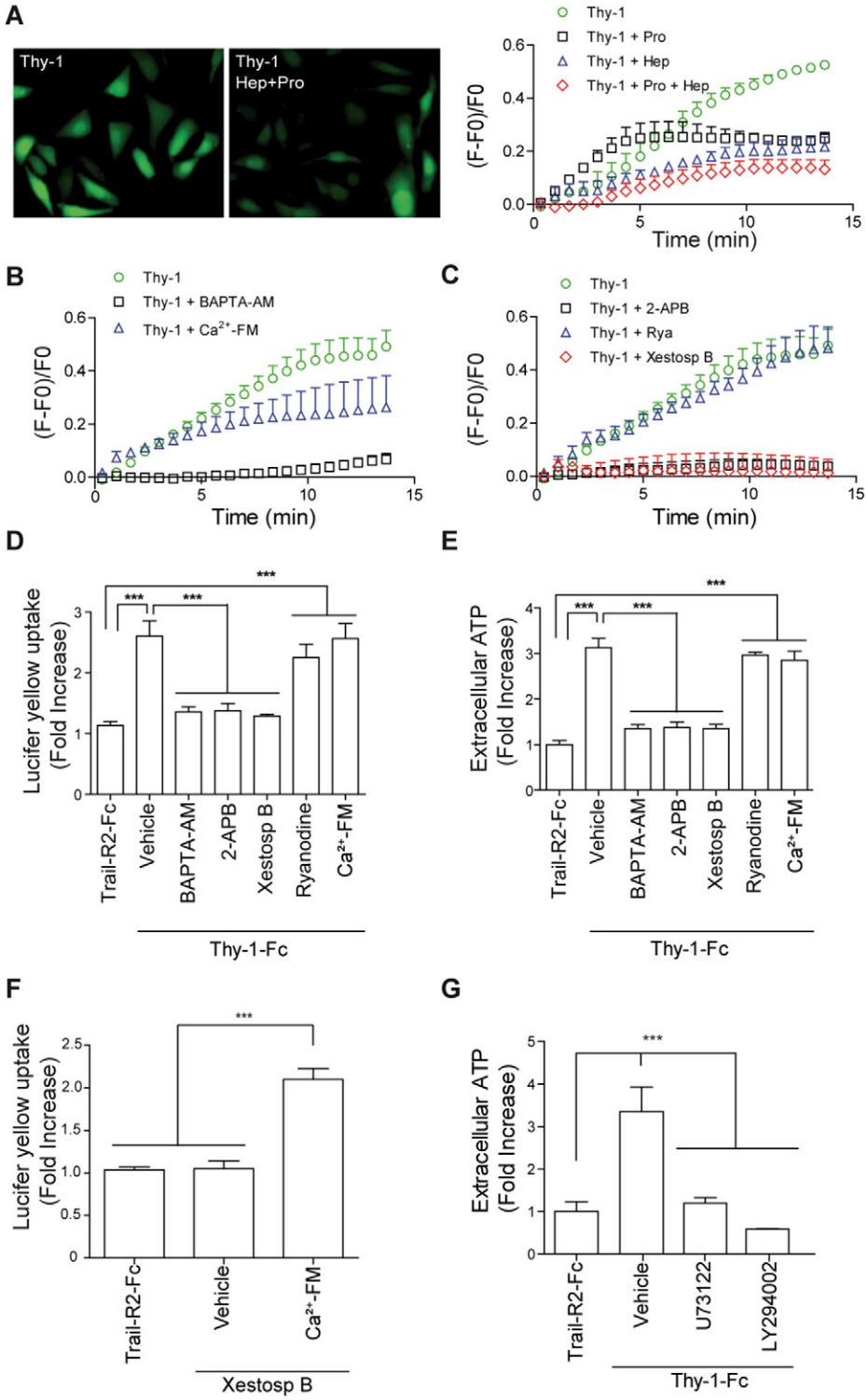

Fig. 4. Intracellular Ca2+ is required for Thy-1-induced ATP release. Changes in the intracellular fluorescence of DITNC1 astrocytes loaded with Fluo4-AM were followed every 2 s. A) Representative microphotographs taken at 12 min and the quantification of intracellular Ca2+ kinetics of DITNC1 astrocytes are shown after stimulation with Thy-1-Fc (green circles) or stimulation following treatment with Heptanol (500 μM, blue triangles), Probenecid (1 mM, black squares) or a combination of both inhibitors for 30 min (red diamonds). B) Intracellular Ca2+ kinetics in DITNC1 astrocytes stimulated with Thy-1-Fc and pre-treated with BAPTA-AM (5 μM for 1 h) or Ca2+-free medium (Ca2+-FM). C) Intracellular Ca2+ kinetics of cells stimulated with Thy-1-Fc and previously treated with 2-APB (5 μM for 1 h), Ryanodine (50 μM for 4 h), or Xestospongine B (5 μM for 4 h). Individual points shown in the graphs correspond to the means ± s.e.m. from three independent experiments. D) Quantification of Lucifer Yellow uptake of DITNC1 astrocytes treated as in B and C. E) Measurement of extracellular ATP in DITNC1 astrocytes treated as in B and C. F) Lucifer Yellow uptake in DITNC1 astrocytes treated with Xestospongine (5 μM) in complete medium or in Ca2+-free medium (Ca2+-FM). G) Measurement of extracellular ATP in DITNC1 astrocytes treated with Thy-1-Fc in the presence of a PLC inhibitor (U73122, 10 μM for 30 min) or a PI3K inhibitor (LY294002, 10 μM for 1 h). ***, $p < 0.001$, estimated from three independent experiments.

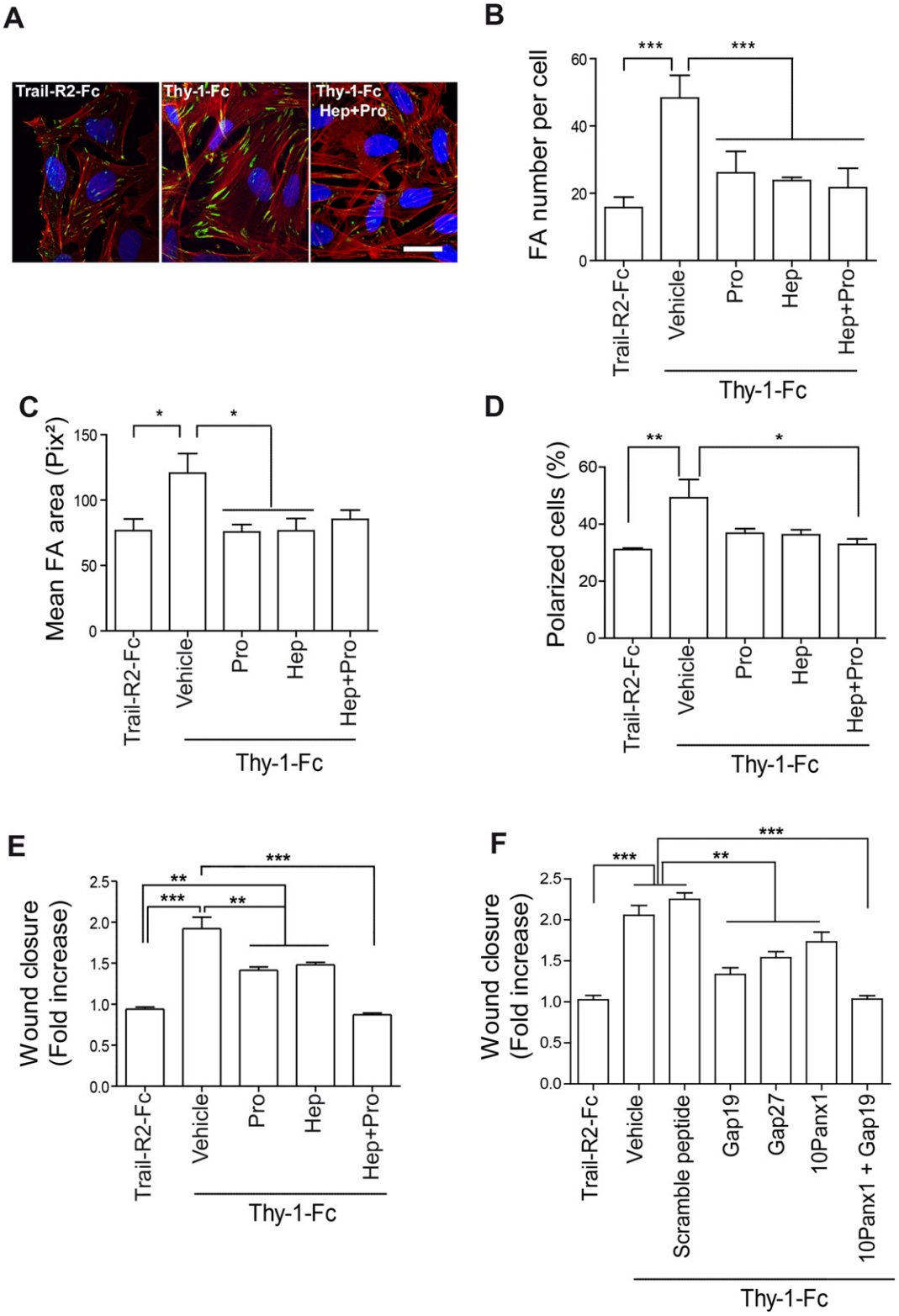

Fig. 5. Thy-1-induced Pannexin-1 and Connexin-43 hemichannel opening is required for astrocyte adhesion, polarization, and migration. DITNC1 astrocytes were stimulated for different periods of time with Thy-1-Fc or treated with Trail-R2-Fc as a control. Where indicated, astrocytes were pre-treated for 30 min with Heptanol (500 μM) or Probenecid (1 mM). A) Representative microphotographs of FAs in DITNC1 astrocytes stimulated with Thy-1-Fc with or without prior treatment for 30 min with Heptanol or Probenecid or treated with Trail-R2-Fc for 15 min. Cells were fixed and stained with anti-vinculin and secondary anti-rabbit IgG antibody conjugated to FITC (green), rhodamine-conjugated Phalloidin (red), and DAPI (blue). Magnification bar = 15 μm. B-C) Quantification of the FA number per cell (B) and average area of FAs (C) observed in DITNC1 astrocytes after the indicated treatments. Values in the graphs represent the means ± s.e.m. determined from at least 50 cells in each experimental condition per experiment using the "Analyze particles" function in ImageJ. D) Cell polarization assay of DITNC1 astrocytes stimulated with Thy-1-Fc or Trail-R2-Fc for 7 h with or without pretreatment with inhibitors as indicated in A. E) Wound-healing assay of DITNC1 astrocytes treated with Thy-1-Fc or Trail-R2-Fc for 24 h with or without prior treatment with inhibitors as indicated in A. F) Scratch assay of DITNC1 cells stimulated as in E, but pre-treatment was performed with vehicle (0.001% DMSO/PBS), Gap19 (100 μM) or Gap27 (300 μM), scramble Gap27 (300 μM), or a mixture of 10panx1 and Gap19 for 30 min. *, $p < 0.05$; **, $p < 0.01$; ***, $p < 0.001$, estimated from three independent experiments.

Ca^{2+} via IP3Rs to allow hemichannel opening, which leads to subsequent ATP release into the medium.

Changes in the intracellular fluorescence of DITNC1 astrocytes loaded with Fluo4-AM were followed every 2 s. A) Representative microphotographs taken at 12 min and the quantification of intracellular Ca^{2+} kinetics of DITNC1 astrocytes are shown after stimulation with Thy-1-Fc (green circles) or stimulation following treatment with Heptanol (500 μM, blue triangles), Probenecid (1 mM, black squares) or a combination of both inhibitors for 30 min (red diamonds). B) Intracellular Ca^{2+} kinetics in DITNC1 astrocytes stimulated with Thy-1-Fc and pre-treated with BAPTA-AM (5 μM for 1 h) or Ca^{2+}-free medium (Ca^{2+}-FM). C) Intracellular Ca^{2+} kinetics of cells stimulated with Thy-1-Fc and previously treated with 2-APB (5 μM for 1 h), Ryanodine (50 μM for 4 h), or Xestospongine B (5 μM for 4 h). Individual points shown in the graphs correspond to the means ± s.e.m. from three independent experiments. D) Quantification of Lucifer Yellow uptake of DITNC1 astrocytes treated as in B and C. E) Measurement of extracellular ATP in DITNC1 astrocytes treated as in B and C. F) Lucifer Yellow uptake in DITNC1 astrocytes treated with Xestospongine (5 μM) in complete medium or in Ca^{2+}-free medium (Ca^{2+}-FM). G) Measurement of extracellular ATP in DITNC1 astrocytes treated with Thy-1-Fc in the presence of a PLC inhibitor (U73122, 10 μM for 30 min) or a PI3K inhibitor (LY294002, 10 μM for 1 h). ***, $p < 0.001$, estimated from three independent experiments.

2.5. ATP released by hemichannels is required for Thy-1-induced cell adhesion, polarization, and migration

As shown previously [20] and in this study, Thy-1-induced P2X7R activation in DITNC1 cells is required to increase cell adhesion, polarization, and migration (Fig. 1). To define the importance of ATP release via hemichannels in these processes, the effects of hemichannel blockers were tested in Thy-1-stimulated astrocytes. The Thy-1-enhanced number of FAs was completely blocked by either Probenecid or Heptanol, and no differences in the number of these structures were observed when cells were treated simultaneously with both inhibitors (Fig. 5A, B). Individually, these inhibitors also prevented the Thy-1-stimulated increase in FA area, while simultaneous treatment with both inhibitors decreased the size of these structures (Fig. 5A, C). Alternatively, although both compounds reduced astrocyte polarization (Fig. 5D) and migration (Fig. 5E) individually, complete inhibition was only achieved when the two reagents were combined. These results indicate that Thy-1 induces ATP release through the opening of both pannexin and connexin hemichannels, which contribute to Thy-1-induced cell adhesion, polarization, and migration.

Because cell migration assays are performed with confluent cell monolayers, we wanted to discard any possible contribution from Connexin-43-formed gap junctions. Therefore, we performed the wound-healing assay in the presence of a specific inhibitor of Connexin-43 hemichannels (Gap19) at a concentration greater than the described IC50, which does not affect gap junctions in astrocytes [54,55]. As observed with Probenecid and Heptanol, Gap19, Gap27 and 10Panx1 partially inhibited cell migration while simultaneous addition of Gap19 and Panx10 blocked cell migration to basal levels (Fig. 5F). The scrambled peptide used as a control had no effect on migration induced by Thy-1 addition.

3. Discussion

Cell adhesion and migration are connected events; therefore, we predicted that the ATP-induced P2X7R activation required for Thy-1-stimulated cell adhesion [20] should also control cell migration. In the present study, we show that ATP release requires the addition of Thy-1 with an intact integrin-binding site and that this ATP release occurs

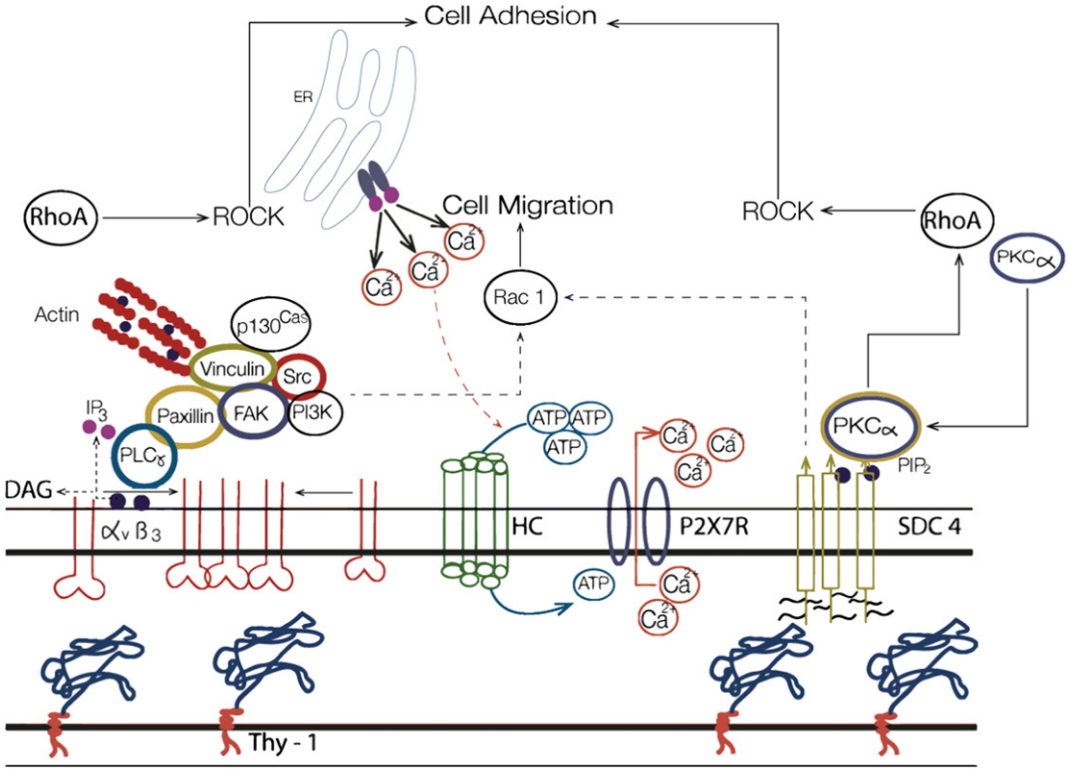

Fig. 6. Signal transduction pathways in astrocyte migration activated by Thy-1 receptors $\alpha_V\beta_3$ integrin and Syndecan-4. $\alpha_V\beta_3$ integrin (receptor 1) engagement by Thy-1 is followed by intracellular signaling pathways that include activation of PI3K and PLCγ, IP3 production, IP3R activation in the ER, increase in cytosolic Ca^{2+}, opening of hemichannels and subsequent ATP release, ATP-mediated P2X7R (receptor 2) activation, Ca^{2+} entry, PKCα activation, and Syndecan-4 (receptor 3)-triggered signaling pathways that include activation of the Rho/ROCK axis with consequent changes in the actin cytoskeleton. Signaling pathways downstream of integrin, which include proteins forming FAs, also control the interplay between RhoA and Rac1 activation and actin remodeling [19].

via a mechanism involving PI3K, PLCγ, IP3R activation, release of Ca^{2+} from the endoplasmic reticulum (ER), and ultimately Pannexin-1 and Connexin-43 hemichannel opening. Extracellular ATP, in turn, induces P2X7R activation, and the resulting influx of Ca^{2+} to the cell interior promotes astrocyte migration (Fig. 6).

The P2X7R has been widely linked in the literature to cell inflammation and cell death, but the connections to cell migration are scarce. Moreover, existing reports concerning the effects of the P2X7R in cell migration are controversial. The P2X7R is reportedly necessary for corneal epithelium migration [56], whereas in fibroblasts, activation of this receptor blocks cell migration in a mitogen-associated protein kinase-dependent manner [57]. In A549 human lung cancer cells, P2X7R activation induces cell migration [22], similar to that described for glioma cells [58], by activating Cathepsin B in a matrix metalloproteinase 9-dependent manner [59]. To the best of our knowledge, there are no reports concerning the relevance of P2X7Rs in astrocyte migration. Most importantly, the data presented herein uncovers a novel mechanism relevant to astrocyte migration, in which receptor transactivation mediated by both Connexin-43 and Pannexin-1 hemichannels establishes a connection between integrin ligation and ATP-induced activation of P2X7Rs.

The controversy described for P2X7Rs in cell migration extends to the BzATP agonist, a pharmacological agent used to stimulate P2X7Rs for the study of cell migration [56–58]. BzATP has been shown to induce, as well as inhibit cell migration, depending on the concentration of the agonist used. BzATP enhances the migration of corneal epithelial cells [60] and C6 glioma cells [58] by activating P2X7R. In a different model, however, BzATP was shown to activate the adenosine receptors, P2X7R and A_{2A}, preventing cell migration when used in low doses while causing the opposite effect when added at high concentrations [61]. Our previous studies showed that BzATP induces astrocyte adhesion [20], and here we show that BzATP also induces cell migration when concentrations are greater than 10 μM. Thus, in our model, BzATP alone is sufficient to mimic the effects of Thy-1-induced signaling downstream of $\alpha_V\beta_3$ integrin and Syndecan-4 engagement [11,19]. A possible interpretation of these results is that continuous release of ATP is required to maintain high local ATP concentrations, which then activate P2X7R and the downstream signaling events required for cell migration. This interpretation would explain how BzATP, a non-hydrolyzable ATP analogue, might suffice to bypass $\alpha_V\beta_3$ integrin and Syndecan-4 engagement.

Interestingly, Thy-1 mutated in the integrin-binding domain [Thy-1(RLE)-Fc], which can still bind to Syndecan-4, did not lead to ATP release, whereas Thy-1 mutated in the HBD [Thy-1(AEAAA)-Fc], which only possesses the integrin-binding site, increased extracellular ATP levels, albeit to a lesser extent and with delayed kinetics compared to wild-type Thy-1 (Fig. 2B). Importantly, neither of these mutated Thy-1 proteins individually stimulates cell adhesion or migration [11,19]; however, the addition of low amounts of BzATP (<10 μM) with the Thy-1 mutant that binds Syndecan-4, suffices to promote cell migration. An interesting possibility is that receptor transactivation involving integrin/ATP/P2X7R stimulation and Ca^{2+} influx further activates Syndecan-4 and downstream signal transduction pathways to promote the continuous ATP release that is required for cells to migrate. This is an intriguing hypothesis involving a feed-forward amplification mechanism that requires further investigation.

Our results also show that the P2X7R-activating ATP is released from Thy-1-stimulated astrocytes through both Connexin-43 and Pannexin-1 hemichannels. Several authors have described ATP release via connexins or pannexins, but evidence suggesting a requirement for both hemichannels in response to a single ligand is limited. ATP release through connexin and pannexin hemichannels has been reported in lung epithelium cells [62]. Additionally, in spinal cord or cerebral astrocytes, ATP release via both hemichannels reportedly also activates P2X7R in response to fibroblast growth factor (FGF) or ultrafine carbon black [32,63]. Importantly though, Abudara and co-workers [32] used Carbexonolone to inhibit both connexins and pannexins simultaneously in spinal cord astrocytes and observed that FGF1 requires both hemichannels to release ATP after 7 h, whereas the increased permeability of the hemichannels detected after 2 h of FGF1 treatment is mediated only by Pannexin-1. Importantly, here we show that the short-term response for cell adhesion (15 min), but not long-term cell migration (24 h), was completely prevented by blocking individual hemichannels (Fig. 5B, C compared with 5E), whereas the combined inhibition of both hemichannels was necessary to reduce cell migration to control levels (Fig. 5E). These results argue that both hemichannels are necessary to activate signaling pathways required for long-term responses (hours), while short-term effects (minutes) involve individual hemichannels.

The present study provides evidence for the participation of hemichannel opening in Thy-1-induced astrocyte adhesion, polarization, and migration. The involvement of Connexin-43 in the migration of various cell types, including neuronal precursor cells, astrocytes, and cancer cells, has been reported [40,41]. In astrocytes, Connexin-43 is necessary for astrocyte migration and proliferation but only upon injury to the central nervous system [40], and no connection between these events and neuron-derived factors has been reported. Alternatively, Pannexin-1 is required for the inflammatory response and the migration of cells from the immune system towards a chemoattractant [42,64]. In these experiments, Pannexin-1 was linked specifically to the cell migration that occurred during regeneration after injury-induced inflammation [42,64]. However, whether Pannexin-1 plays a role in cell migration under non-inflammatory conditions is less clear, although some recently emerging evidence suggests that this is the case [43]. The results reported in our present study are novel in this sense because they describe how the neuronal protein, Thy-1, via integrin-dependent opening of Connexin-43 and Pannexin-1 hemichannels, allows ATP release that, in turn, activates P2X7R. In doing so, this sequence of events links Thy-1-induced integrin signaling and astrocyte migration to P2X7R transactivation via ATP release.

The additional data provided here demonstrate that Thy-1-induced hemichannel opening requires the release of intracellular Ca^{2+} from the ER through IP3R channels. Specifically, we show that PI3K and PLCγ activation lie upstream of ATP release induced by Thy-1-$\alpha_V\beta_3$ integrin-binding. Additionally, our previous results implicate PLCγ in Thy-1-induced RhoA activation and astrocyte adhesion [20]. We have also reported that PI3K activation occurs downstream of $\alpha_V\beta_3$ integrin/FAK autophosphorylation [19]. By assessing Akt phosphorylation as an indirect indicator of PI3K activation, we observed that Thy-1 containing the integrin-binding site but lacking the region for Syndecan-4-binding increased phosphorylation of Akt and that this event was precluded by the PI3K inhibitor, LY294002 [19]. Importantly, active PI3K increases levels of phosphatidylinositol 3,4,5-trisphosphate at the plasma membrane, providing sites for recruitment of PLCγ [65,66]. Then, PLCγ activated downstream of the $\alpha_V\beta_3$ integrin/FAK/PI3K signaling cascade increases IP3 levels to stimulate IP3Rs in the ER and increase intracellular $[Ca^{2+}]$.

Reportedly, augmented cytosolic Ca^{2+} is necessary for hemichannel opening. Connexin-43 hemichannels alter their permeability in response to changes in intracellular Ca^{2+} levels by either direct binding of Ca^{2+} to the hemichannel or via Ca^{2+}/calmodulin-dependent activation [55,67]. Additionally, cytosolic Ca^{2+} has been reported to induce Pannexin-1 opening [68], whereas low extracellular Ca^{2+} concentrations increase the binding and activity of the P2X7R-Pannexin-1 complex [69]. Moreover, Ca^{2+} activates Ca^{2+}/calmodulin-dependent kinases and/or conventional PKCs that, like calmodulin, modify hemichannel function [70,71]. However, the details of the molecular mechanisms by which enhanced $[Ca^{2+}]_i$ might regulate hemichannel opening upon stimulation of astrocytes with Thy-1 remain to be defined.

Our recently reported data indicate that Thy-1-induced cell adhesion, polarization, and migration require the interaction of Thy-1 not only with $\alpha_V\beta_3$ integrin, but also with Syndecan-4 [11,19]. Interestingly,

Syndecan-4 has been suggested to form a complex with PKCα to further activate RhoA and promote morphological changes and cell adhesion [11,72,73]. Given that the activation of this conventional PKC isoform depends on calcium [74] and that integrin engagement is followed by ATP/P2X7R-mediated Ca^{2+} influx into the cytosol [20], PKCα may be activated as a consequence of such Ca^{2+} entry (Fig. 6). Indeed, PKCα membrane translocation, an important step for PKC activation, via P2X7R-induced Ca^{2+} elevation has been reported in osteoclasts [75]. Importantly, to form a complex with Syndecan-4, PKCα must translocate to the plasma membrane [73]. Thus, the activation of PKCα in a canonical manner, downstream of integrin/P2X7R, could generate a transient membrane-bound pool of PKCα required to form stable complexes with Syndecan-4 (Fig. 6). Taken together, our results indicate that, in astrocytes stimulated with Thy-1, integrin-dependent events might be activated prior to those triggered by Syndecan-4 in a sequential manner. It should be noted that the cells utilized in the present study also express Syndecan-1 [11], which is implicated in cell migration [76]. The focus on Syndecan-4 was driven by our previous results implicating Syndecan-4 and PKCα in adhesion and migration [11,19]. Moreover, the Syndecan-4 interactome is considerably more complex than the Syndecan-1 interactome due to the formation of a ternary complex between Syndecan-4, PIP2, and PKCα [77]. Therefore, we interpreted the participation of PKCα in our system as indicative of a prevalent role for Syndecan-4 rather than Syndecan-1 in astrocyte migration. Nonetheless, Syndecan-1 participation in astrocyte migration cannot be ruled out.

In summary, we suggest a receptor transactivation sequence (Fig. 6), whereby $\alpha_v\beta_3$ integrin (receptor 1) engagement is followed by the activation of a complex signaling sequence that includes PI3K and PLCγ activation, IP3 production, IP3R activation, an increase in cytosolic Ca^{2+}, opening of hemichannels and subsequent ATP release, ATP-mediated P2X7R (receptor 2) activation, Ca^{2+} entry, PKCα activation, and Syndecan-4 (receptor 3)-triggered signaling pathways.

4. Materials and methods

4.1. Culture of DITNC1 cells

The DITNC1 astrocyte cell line (ATCC, CRL-2005) was originally obtained from primary cultures of rat diencephalons. Astrocytes were cultured in RPMI medium (Gibco, Life Technologies, Grand Island, NY) with 5% fetal bovine serum (FBS), 0.1 mM 2-mercaptoethanol, 100 U/ml penicillin, and 100 μg/ml streptomycin (complete medium).

4.2. Thy-1-Fc and Trail-R2-Fc preparation

Thy-1-Fc (wild-type and mutants) and Trail-R2-Fc fusion proteins were obtained as described previously [11,14]. Proteins (2 μg/lane) were separated by SDS-polyacrylamide gel electrophoresis (SDS-PAGE) under non-reducing conditions and stained with Coomassie Brilliant blue. Thy-1-Fc and Trail-R2-Fc proteins were incubated with Protein A in a 10:1 ratio with gentle rotation for 1 h at 4 °C prior to their use. Astrocyte stimulation was performed by adding 1 μg of fusion protein per 50,000 cells [13]. Trail-R2-Fc is a fusion protein of the receptor for the soluble apoptosis-inducing ligand, Trail [78], and it is used in these assays as a negative control for possible side effects caused by the Fc portion of the Thy-1 fusion proteins.

4.3. Wound-healing assay

DITNC1 cells were seeded in 24-well plates (100,000 cells per well), and after 24 h, two parallel wounds were introduced with a micropipette tip. Detached cells were washed away, and after 30 min of starvation, cells were stimulated with 4 μg of either Thy-1-Fc or Trail-R2-Fc (negative control) for 24 h; both proteins were coupled to Protein A as indicated above. The effect of the Thy-1-Fc mutants was tested either separately or in combination by adding both Thy-1(RLE)-Fc and Thy-1(AEAAA)-Fc to the Protein A coupling mix. Alternatively, migration was evaluated after treating the cells with various concentrations of BzATP in serum-free medium for 24 h with or without mutated Thy-1 proteins. Where indicated, BBG (5 μM), A438079 (100 nM), and Apyrase (3 U/ml), Probenecid (1 mM), Heptanol (500 μM), Gap19 (100 μM), Gap27 (300 μM), or scrambled peptide (300 μM) were added 30 min prior to stimulation and left for the next 24 h. These experiments were also performed using DITNC1 cells transiently transfected with specific siRNA against P2X7R (Dharmacon, Lafayette, CO) or the indicated negative siRNA control using the siPORT Amine transfection reagent (Ambion, Thermo Fischer Scientific, Rockford, IL) as previously reported [20]. Images used to quantify the cell-free area were obtained at 0 and 24 h as described [19].

4.4. Polarity assay

Astrocytes were seeded on 12-mm coverslips (50,000 cells per coverslip), prepared and treated as for wound-healing assays, but were stimulated with Protein A-conjugated Thy-1-Fc, Trail-R2-Fc, or 100 μM BzATP for 7 h. Astrocytes were then fixed for 10 min with 4% paraformaldehyde, permeabilized, and blocked as described previously [45]. Cells were then incubated at 37 °C with anti-giantin antibody (Covance Research Products, Denver, PA) for 1 h, followed by secondary antibody coupled to FITC (Jackson ImmunoResearch Laboratories, Inc., West Grove, PA) and Rhodamine-conjugated Phalloidin (Sigma-Aldrich Co., Saint Louis, MO) for 1 h to stain for F-actin. DAPI (0.025 μg/ml) was used to stain the nucleus. Coverslips were mounted on slides as described previously [19], and samples were observed using a Disk Scanning Unit-IX81 Spinning disk confocal microscope (Olympus Corp.). Cells were considered polarized when the Golgi apparatus was located in the perinuclear area and oriented towards the cell-free zone within a 120° angle (see scheme in Fig. 1C). DITNC1 cells were stimulated as described previously [19]. One hundred cells were monitored per condition, and cell polarization was evaluated as the percentage of cells along the wound border exhibiting polarized Golgi structures [45].

4.5. Extracellular ATP measurements

DITNC1 astrocytes (50,000) in 50 μl were left in serum-free media containing 100 μM of the exonuclease inhibitor, Ebselen, for 30 min at 37 °C. Before stimulation with Thy-1-Fc:Protein A (10 min or as indicated for kinetic analyses) where indicated, cells were incubated with Heptanol (500 μM), Probenecid (1 mM), or a combination of both inhibitors; the exocytosis inhibitors, Brefeldine A (3 μg/ml for 4 h) or Bafilomycin A (1 μM for 4 h); the hemichannel-blocking peptides, 10panx1 (100 μM), E1B (100 μM), Gap 26 (300 μM), or Gap27 (300 μM), for 30 min; the IP3R blockers, 2-APB (5 μM for 1 h) or Xestospongine B (5 μM for 4 h); Ryanodine (50 μM for 4 h); BAPTA-AM (5 μM for 1 h); U73122 (10 μM for 30 min); or LY294002 (10 μM for 1 h). Afterwards, cells were centrifuged for 5 min at 800 ×*g*. The supernatants were then incubated in the dark with 20 μl of the CellTiter-Glo (Promega, Madison, WI) reaction mix for 40 min. Luminescence intensity was determined in a Synergy2 multi-mode reader (Biotek Instruments, Inc., Vermont), and the values were interpolated using a calibration curve obtained with different ATP concentrations (0.01, 0.1, 1, and 10 μM). Furthermore, these experiments also included DITNC1 cells transiently transfected with specific siRNA against Syndecan-4 (Ambion), β_3 integrin (Ambion), or the indicated negative siRNA control using the Amaxa Nucleofector system (Lonza, Cologne, Germany).

4.6. Lucifer Yellow uptake

DITNC1 astrocytes (400,000 cells) were seeded on 25-mm coverslips and left to adhere for 24 h. Cells were then treated with the indicated inhibitors (as for ATP measurements) prior to stimulating with Thy-1-Fc or Trail-R2-Fc coupled to Protein A for 10 min. After stimulation, the cells were incubated at 37 °C with 0.5 mg/ml Lucifer Yellow in Ringer Solution (155 mM NaCl, 4.5 mM KCl, 2 mM $CaCl_2$, 1 mM $MgCl_2$, 10 mM glucose, and 5 mM Hepes pH 7.4) for 10 min and then washed twice with the same solution. Lucifer Yellow fluorescence intensity was quantified in 100 cells per condition in relative units, using the region of interest (ROI) plug-in in the ImageJ software (National Institutes of Health, Bethesda, MD, http://imagej.nih.gov/ij/). The probe was excited at 458 nm, and emission between 500–530 nm was quantified.

4.7. Western blot analysis

Protein extracts were prepared in lysis buffer (150 mM NaCl, 0.1% SDS, 0.25% sodium deoxycholate, 1% Triton-X100, and 50 mM Tris pH 7.4,) supplemented with protease and phosphatase inhibitor cocktails (Biotool, Houston, TX). Extracts were electrophoretically separated in 10% SDS-PAGE gels and transferred to nitrocellulose (Millipore, Billerica, USA). The nitrocellulose was blocked with 5% w/v nonfat, dry milk in PBS containing 0.1% Tween-20 and then incubated with the primary antibodies: anti-Connexin-43 (1:500; Santa Cruz Biotechnologies Dallas, TX) or anti-Pannexin-1 (1:500; Santa Cruz Biotechnologies). The membrane was then washed and incubated with the horseradish peroxidase-conjugated goat anti-rabbit IgG (1:5000; Abbexa, Cambridge, UK) or donkey anti-goat IgG (1:5000; Abbexa) antibodies for 1 h at room temperature. Bands were visualized with a chemiluminescence kit (Pierce, Thermo Scientific, Rockford, IL), according to the manufacturer's instructions.

4.8. Measurement of intracellular calcium kinetics

Astrocytes were seeded on 25-mm coverslips (400,000 cells) and left to adhere for 24 h. The cells were then incubated for 40 min with 5 μM Fluo-4-AM in Ringer solution at 37 °C. The cells were washed and left in the same solution. Astrocytes were treated with the hemichannel blockers, Heptanol (500 μM), Probenecid (1 mM), or a mixture of both inhibitors for 30 min; the IP3R blockers, 2-APB (5 μM for 1 h) or Xestospongine B (5 μM for 4 h); Ryanodine (50 μM for 4 h); or BAPTA-AM (5 μM for 1 h). Images were acquired at 2-second intervals with an XM10 camera (Olympus Corp.). Thy-1-Fc or Trail-R2-Fc, both coupled to Protein A, were added after 40 s, and the fluorescence was recorded for 15 min. Fluorescence intensity was quantified in 100 cells per condition using ImageJ. The results were expressed as $(F—F_0)/F_0$, where F is the change in fluorescence and F_0 is the basal fluorescence.

4.9. Focal adhesion assay

DITNC1 cells were seeded on 12-mm coverslips and left to adhere for 24 h. The cells were then pre-treated with the hemichannel blockers, Heptanol (500 μM), Probenecid (1 mM), or a combination of both inhibitors for 30 min and stimulated with Thy-1-Fc-Protein A or the control protein for 15 min. Astrocytes were then washed and fixed for 10 min with 4% paraformaldehyde, permeabilized for 10 min, and blocked for 1 h with 2% bovine serum albumin (BSA). The cells were then incubated with antibodies for 1 h at 37 °C. Anti-vinculin, rhodamine-conjugated Phalloidin, and DAPI (0.025 μg/ml) were used to stain for focal adhesions, F-actin, and nuclei, respectively. Quantification of focal adhesion area and number was performed following previously described protocols [11].

4.10. Indirect immunofluorescence assay

DITNC1 cells seeded on 12-mm coverslips and left to adhere for 24 h were then washed and fixed as indicated for the Focal adhesion assay. Afterward, cells were stained with anti-Connexin-43 (1:200) or anti-Pannexin-1 (1:200) antibodies followed by secondary antibodies (1:500) conjugated to IF488 (green) or IF594 (red), respectively (Abbexa), and DAPI (0.025 μg/ml) (blue). Samples were analyzed using a confocal microscope C2+ (Nikon), with 60X/1.40 objective and NIS-Elements software.

4.11. Statistical analysis

The results are shown as the means ± standard error of the mean (s.e.m.) for $n = 3$ or more experiments. The results were analyzed using one-way ANOVA tests and Tukey post-tests. Statistical significance was set at $p < 0.05$.

Author contributions

AA and LL designed and executed the experiments, interpreted the data, and prepared the article. RLC, MK, FB and AC helped to execute the experiments and interpreted the data. RLC and FB additionally prepared the data for publication. PS and AFGQ helped to interpret the data and prepare the article.

Competing interests

The authors declare no conflicts of interest.

Transparency document

The Transparency document associated with this article can be found, in online version.

Acknowledgements

This study was supported by the following grants: FONDECYT #1110149 and #1150744 (LL), #1090071 and #1130250 (AFGQ), #3140471 (AC), and #3140460 (RL); CONICYT #21090323 (AA) and #21130008 (FB); CONICYT-FONDAP #15130011 (AFGQ); Anillos #ACT1111 (AFGQ); Iniciativas Científicas Milenio #P09-015-F (LL, RL, AA, FB and AC); and Grants of the Swiss National Science Foundation #310030_156961 (PS). The authors wish to thank Dr. Juan Carlos Saez (P. Universidad Catolica de Chile) for helpful discussions.

References

[1] K. Burridge, K. Fath, T. Kelly, G. Nuckolls, C. Turner, Focal adhesions: transmembrane junctions between the extracellular matrix and the cytoskeleton, Annu. Rev. Cell Biol. 4 (1988) 487–525.
[2] B. Geiger, Cytoskeleton-associated cell contacts, Curr. Opin. Cell Biol. 1 (1989) 103–109.
[3] K.R. Fath, C.J. Edgell, K. Burridge, The distribution of distinct integrins in focal contacts is determined by the substratum composition, J. Cell Sci. 92 (1989) 67–75.
[4] A.J. Ridley, M.A. Schwartz, K. Burridge, R.A. Firtel, M.H. Ginsberg, G. Borisy, J.T. Parsons, A.R. Horwitz, Cell migration: integrating signals from front to back, Science 302 (2003) 1704–1709.
[5] B. Wehrle-Haller, B.A. Imhof, Actin, microtubules and focal adhesion dynamics during cell migration, Int. J. Biochem. Cell Biol. 35 (2003) 39–50.
[6] R. Zaidel-Bar, C. Ballestrem, Z. Kam, B. Geiger, Early molecular events in the assembly of matrix adhesions at the leading edge of migrating cells, J. Cell Sci. 116 (2003) 4605–4613.
[7] S. Manes, E. Mira, C. Gomez-Mouton, R.A. Lacalle, C. Martinez, Cells on the move: a dialogue between polarization and motility, IUBMB Life 49 (2000) 89–96.
[8] B. Geiger, K.M. Yamada, Molecular architecture and function of matrix adhesions, Cold Spring Harb. Perspect. Biol. 3 (2011) (pii: a005033).
[9] R. Zaidel-Bar, B. Geiger, The switchable integrin adhesome, J. Cell Sci. 123 (2010) 1385–1388.
[10] A. Woods, J.R. Couchman, Syndecans: synergistic activators of cell adhesion, Trends Cell Biol. 8 (1998) 189–192.

[11] A.M. Avalos, A.D. Valdivia, N. Munoz, R. Herrera-Molina, J.C. Tapia, S. Lavandero, M. Chiong, K. Burridge, P. Schneider, A.F. Quest, L. Leyton, Neuronal Thy-1 induces astrocyte adhesion by engaging syndecan-4 in a cooperative interaction with $\alpha_V\beta_3$ integrin that activates PKCα and RhoA, J. Cell Sci. 122 (2009) 3462–3471.
[12] M.D. Bass, R.C. Williamson, R.D. Nunan, J.D. Humphries, A. Byron, M.R. Morgan, P. Martin, M.J. Humphries, A syndecan-4 hair trigger initiates wound healing through caveolin- and RhoG-regulated integrin endocytosis, Dev. Cell 21 (2011) 681–693.
[13] T. Hermosilla, D. Munoz, R. Herrera-Molina, A. Valdivia, N. Munoz, S.U. Nham, P. Schneider, K. Burridge, A.F. Quest, L. Leyton, Direct Thy-1/$\alpha_V\beta_3$ integrin interaction mediates neuron to astrocyte communication, Biochim. Biophys. Acta 1783 (2008) 1111–1120.
[14] L. Leyton, P. Schneider, C.V. Labra, C. Ruegg, C.A. Hetz, A.F. Quest, C. Bron, Thy-1 binds to integrin β_3 on astrocytes and triggers formation of focal contact sites, Curr. Biol. 11 (2001) 1028–1038.
[15] V.F. Fiore, L. Ju, Y. Chen, C. Zhu, T.H. Barker, Dynamic catch of a Thy-1-$\alpha_5\beta_1$ + syndecan-4 trimolecular complex, Nat. Commun. 5 (2014) 4886.
[16] A. Wetzel, T. Chavakis, K.T. Preissner, M. Sticherling, U.F. Haustein, U. Anderegg, A. Saalbach, Human Thy-1 (CD90) on activated endothelial cells is a counterreceptor for the leukocyte integrin Mac-1 (CD11b/CD18), J. Immunol. 172 (2004) 3850–3859.
[17] Y. Zhou, J.S. Hagood, B. Lu, W.D. Merryman, J.E. Murphy-Ullrich, Thy-1-integrin $\alpha_V\beta_5$ interactions inhibit lung fibroblast contraction-induced latent transforming growth factor-β_1 activation and myofibroblast differentiation, J. Biol. Chem. 285 (2010) 22382–22393.
[18] A.M. Avalos, W.T. Arthur, P. Schneider, A.F. Quest, K. Burridge, L. Leyton, Aggregation of integrins and RhoA activation are required for Thy-1-induced morphological changes in astrocytes, J. Biol. Chem. 279 (2004) 39139–39145.
[19] M. Kong, N. Munoz, A. Valdivia, A. Alvarez, R. Herrera-Molina, A. Cardenas, P. Schneider, K. Burridge, A.F. Quest, L. Leyton, Thy-1-mediated cell-cell contact induces astrocyte migration through the engagement of $\alpha_V\beta_3$ integrin and syndecan-4, Biochim. Biophys. Acta 1833 (2013) 1409–1420.
[20] M. Henriquez, R. Herrera-Molina, A. Valdivia, A. Alvarez, M. Kong, N. Munoz, V. Eisner, E. Jaimovich, P. Schneider, A.F. Quest, L. Leyton, ATP release due to Thy-1-integrin binding induces P2X7-mediated calcium entry required for focal adhesion formation, J. Cell Sci. 124 (2011) 1581–1588.
[21] S. Coco, F. Calegari, E. Pravettoni, D. Pozzi, E. Taverna, P. Rosa, M. Matteoli, C. Verderio, Storage and release of ATP from astrocytes in culture, J. Biol. Chem. 278 (2003) 1354–1362.
[22] E. Takai, M. Tsukimoto, H. Harada, K. Sawada, Y. Moriyama, S. Kojima, Autocrine regulation of TGF-β_1-induced cell migration by exocytosis of ATP and activation of P2 receptors in human lung cancer cells, J. Cell Sci. 125 (2012) 5051–5060.
[23] M.L. Cotrina, J.H. Lin, A. Alves-Rodrigues, S. Liu, J. Li, H. Azmi-Ghadimi, J. Kang, C.C. Naus, M. Nedergaard, Connexins regulate calcium signaling by controlling ATP release, Proc. Natl. Acad. Sci. U. S. A. 95 (1998) 15735–15740.
[24] H.K. Eltzschig, T. Eckle, A. Mager, N. Kuper, C. Karcher, T. Weissmuller, K. Boengler, R. Schulz, S.C. Robson, S.P. Colgan, ATP release from activated neutrophils occurs via Connexin-43 and modulates adenosine-dependent endothelial cell function, Circ. Res. 99 (2006) 1100–1108.
[25] C. Giaume, C. Fromaget, A. el Aoumari, J. Cordier, J. Glowinski, D. Gros, Gap junctions in cultured astrocytes: single-channel currents and characterization of channel-forming protein, Neuron 6 (1991) 133–143.
[26] J. Kang, N. Kang, D. Lovatt, A. Torres, Z. Zhao, J. Lin, M. Nedergaard, Connexin-43 hemichannels are permeable to ATP, J. Neurosci. 28 (2008) 4702–4711.
[27] P. Luckprom, K. Kanjanamekanant, P. Pavasant, Role of Connexin-43 hemichannels in mechanical stress-induced ATP release in human periodontal ligament cells, J. Periodontal Res. 46 (2011) 607–615.
[28] J.A. Orellana, E. Diaz, K.A. Schalper, A.A. Vargas, M.V. Bennett, J.C. Saez, Cation permeation through Connexin-43 hemichannels is cooperative, competitive and saturable with parameters depending on the permeant species, Biochem. Biophys. Res. Commun. 409 (2011) 603–609.
[29] P. Pelegrin, A. Surprenant, Pannexin-1 mediates large pore formation and interleukin-1β release by the ATP-gated P2X7 receptor, EMBO J. 25 (2006) 5071–5082.
[30] S.O. Suadicani, R. Iglesias, J. Wang, G. Dahl, D.C. Spray, E. Scemes, ATP signaling is deficient in cultured Pannexin-1-null mouse astrocytes, Glia 60 (2012) 1106–1116.
[31] M.V. Bennett, J.M. Garre, J.A. Orellana, F.F. Bukauskas, M. Nedergaard, J.C. Saez, Connexin and pannexin hemichannels in inflammatory responses of glia and neurons, Brain Res. 1487 (2012) 3–15.
[32] J.M. Garre, M.A. Retamal, P. Cassina, L. Barbeito, F.F. Bukauskas, J.C. Saez, M.V. Bennett, V. Abudara, FGF-1 induces ATP release from spinal astrocytes in culture and opens pannexin and connexin hemichannels, Proc. Natl. Acad. Sci. U. S. A. 107 (2010) 22659–22664.
[33] M.V. Bennett, J.E. Contreras, F.F. Bukauskas, J.C. Saez, New roles for astrocytes: gap junction hemichannels have something to communicate, Trends Neurosci. 26 (2003) 610–617.
[34] J.E. Contreras, H.A. Sanchez, E.A. Eugenin, D. Speidel, M. Theis, K. Willecke, F.F. Bukauskas, M.V. Bennett, J.C. Saez, Metabolic inhibition induces opening of unapposed Connexin-43 gap junction hemichannels and reduces gap junctional communication in cortical astrocytes in culture, Proc. Natl. Acad. Sci. U. S. A. 99 (2002) 495–500.
[35] H. Li, T.F. Liu, A. Lazrak, C. Peracchia, G.S. Goldberg, P.D. Lampe, R.G. Johnson, Properties and regulation of gap junctional hemichannels in the plasma membranes of cultured cells, J. Cell Biol. 134 (1996) 1019–1030.
[36] Z.C. Ye, M.S. Wyeth, S. Baltan-Tekkok, B.R. Ransom, Functional hemichannels in astrocytes: a novel mechanism of glutamate release, J. Neurosci. 23 (2003) 3588–3596.
[37] G. Sahu, S. Sukumaran, A.K. Bera, Pannexins form gap junctions with electrophysiological and pharmacological properties distinct from connexins, Sci. Rep. 4 (2014) 4955.
[38] F. Vanden Abeele, G. Bidaux, D. Gordienko, B. Beck, Y.V. Panchin, A.V. Baranova, D.V. Ivanov, R. Skryma, N. Prevarskaya, Functional implications of calcium permeability of the channel formed by Pannexin-1, J. Cell Biol. 174 (2006) 535–546.
[39] R. Francis, X. Xu, H. Park, C.J. Wei, S. Chang, B. Chatterjee, C. Lo, Connexin-43 modulates cell polarity and directional cell migration by regulating microtubule dynamics, PLoS One 6 (2011), e26379.
[40] B. Homkajorn, N.R. Sims, H. Muyderman, Connexin-43 regulates astrocytic migration and proliferation in response to injury, Neurosci. Lett. 486 (2010) 197–201.
[41] P. Kameritsch, K. Pogoda, U. Pohl, Channel-independent influence of connexin-43 on cell migration, Biochim. Biophys. Acta 1818 (2012) 1993–2001.
[42] Y. Bao, Y. Chen, C. Ledderose, L. Li, W.G. Junger, Pannexin-1 channels link chemoattractant receptor signaling to local excitation and global inhibition responses at the front and back of polarized neutrophils, J. Biol. Chem. 288 (2013) 22650–22657.
[43] A.K. Boyce, L.E. Wicki-Stordeur, L.A. Swayne, Powerful partnership: crosstalk between Pannexin-1 and the cytoskeleton, Front. Physiol. 5 (2014) 27.
[44] S. Penuela, L. Gyenis, A. Ablack, J.M. Churko, A.C. Berger, D.W. Litchfield, J.D. Lewis, D.W. Laird, Loss of Pannexin-1 attenuates melanoma progression by reversion to a melanocytic phenotype, J. Biol. Chem. 287 (2012) 29184–29193.
[45] H. Urra, V.A. Torres, R.J. Ortiz, L. Lobos, M.I. Diaz, N. Diaz, S. Hartel, L. Leyton, A.F. Quest, Caveolin-1-enhanced motility and focal adhesion turnover require tyrosine-14 but not accumulation to the rear in metastatic cancer cells, PLoS One 7 (2012), e33085.
[46] A. Dinter, E.G. Berger, Golgi-disturbing agents, Histochem. Cell Biol. 109 (1998) 571–590.
[47] J.A. Orellana, D.E. Hernandez, P. Ezan, V. Velarde, M.V. Bennett, C. Giaume, J.C. Saez, Hypoxia in high glucose followed by reoxygenation in normal glucose reduces the viability of cortical astrocytes through increased permeability of Connexin-43 hemichannels, Glia 58 (2010) 329–343.
[48] R. Dermietzel, Y. Gao, E. Scemes, D. Vieira, M. Urban, M. Kremer, M.V. Bennett, D.C. Spray, Connexin-43 null mice reveal that astrocytes express multiple connexins, Brain Res. Brain Res. Rev. 32 (2000) 45–56.
[49] R. Iglesias, G. Dahl, F. Qiu, D.C. Spray, E. Scemes, Pannexin-1: the molecular substrate of astrocyte "hemichannels", J. Neurosci. 29 (2009) 7092–7097.
[50] R.J. Thompson, B.A. Macvicar, Connexin and pannexin hemichannels of neurons and astrocytes, Channels (Austin) 2 (2008) 81–86.
[51] J.L. Solan, P.D. Lampe, Connexin phosphorylation as a regulatory event linked to gap junction channel assembly, Biochim. Biophys. Acta 1711 (2005) 154–163.
[52] G. Meissner, Ryanodine activation and inhibition of the Ca^{2+} release channel of sarcoplasmic reticulum, J. Biol. Chem. 261 (1986) 6300–6306.
[53] C.E. Stout, J.L. Costantin, C.C. Naus, A.C. Charles, Intercellular calcium signaling in astrocytes via ATP release through connexin hemichannels, J. Biol. Chem. 277 (2002) 10482–10488.
[54] V. Abudara, J. Bechberger, M. Freitas-Andrade, M. De Bock, N. Wang, G. Bultynck, C.C. Naus, L. Leybaert, C. Giaume, The Connexin-43 mimetic peptide Gap19 inhibits hemichannels without altering gap junctional communication in astrocytes, Front. Cell. Neurosci. 8 (2014) 306.
[55] N. Wang, M. De Bock, E. Decrock, M. Bol, A. Gadicherla, G. Bultynck, L. Leybaert, Connexin targeting peptides as inhibitors of voltage- and intracellular Ca^{2+}-triggered Connexin-43 hemichannel opening, Neuropharmacology 75 (2013) 506–516.
[56] C. Mayo, R. Ren, C. Rich, M.A. Stepp, V. Trinkaus-Randall, Regulation by P2X7: epithelial migration and stromal organization in the cornea, Invest. Ophthalmol. Vis. Sci. 49 (2008) 4384–4391.
[57] S. Kumagai, K. Matsui, H. Kawaguchi, T. Yamashita, T. Mohri, Y. Fujio, H. Nakayama, Cathelicidin antimicrobial peptide inhibits fibroblast migration via P2X7 receptor signaling, Biochem. Biophys. Res. Commun. 437 (2013) 609–614.
[58] W. Wei, J.K. Ryu, H.B. Choi, J.G. McLarnon, Expression and function of the P2X7 receptor in rat C6 glioma cells, Cancer Lett. 260 (2008) 79–87.
[59] N. Murphy, M.A. Lynch, Activation of the P2X7 receptor induces migration of glial cells by inducing cathepsin B degradation of tissue inhibitor of metalloproteinase 1, J. Neurochem. 123 (2012) 761–770.
[60] C. Mankus, C. Rich, M. Minns, V. Trinkaus-Randall, Corneal epithelium expresses a variant of P2X7 receptor in health and disease, PLoS One 6 (2011), e28541.
[61] J.Z. Zhou, M.A. Riquelme, X. Gao, L.G. Ellies, L.Z. Sun, J.X. Jiang, Differential impact of adenosine nucleotides released by osteocytes on breast cancer growth and bone metastasis, Oncogene 34 (2015) 1831–1842.
[62] K. Richter, K.P. Kiefer, B.A. Grzesik, W.G. Clauss, M. Fronius, Hydrostatic pressure activates ATP-sensitive K+ channels in lung epithelium by ATP release through pannexin and connexin hemichannels, FASEB J. 28 (2014) 45–55.
[63] H. Wei, F. Deng, Y. Chen, Y. Qin, Y. Hao, X. Guo, Ultrafine carbon black induces glutamate and ATP release by activating connexin and pannexin hemichannels in cultured astrocytes, Toxicology 323 (2014) 32–41.
[64] H.P. Makarenkova, V.I. Shestopalov, The role of pannexin hemichannels in inflammation and regeneration, Front. Physiol. 5 (2014) 63.
[65] M. Falasca, S.K. Logan, V.P. Lehto, G. Baccante, M.A. Lemmon, J. Schlessinger, Activation of phospholipase Cγ by PI 3-kinase-induced PH domain-mediated membrane targeting, EMBO J. 17 (1998) 414–422.

[66] L.E. Rameh, S.G. Rhee, K. Spokes, A. Kazlauskas, L.C. Cantley, L.G. Cantley, Phosphoinositide 3-kinase regulates phospholipase Cγ-mediated calcium signaling, J. Biol. Chem. 273 (1998) 23750–23757.
[67] C. Peracchia, Chemical gating of gap junction channels; roles of calcium, pH and calmodulin, Biochim. Biophys. Acta 1662 (2004) 61–80.
[68] S. Locovei, J. Wang, G. Dahl, Activation of Pannexin-1 channels by ATP through P2Y receptors and by cytoplasmic calcium, FEBS Lett. 580 (2006) 239–244.
[69] V. Poornima, M. Madhupriya, S. Kootar, G. Sujatha, A. Kumar, A.K. Bera, P2X7 receptor-Pannexin-1 hemichannel association: effect of extracellular calcium on membrane permeabilization, J. Mol. Neurosci. 46 (2012) 585–594.
[70] X. Bao, S.C. Lee, L. Reuss, G.A. Altenberg, Change in permeant size selectivity by phosphorylation of Connexin-43 gap-junctional hemichannels by PKC, Proc. Natl. Acad. Sci. U. S. A. 104 (2007) 4919–4924.
[71] E. De Vuyst, N. Wang, E. Decrock, M. De Bock, M. Vinken, M. Van Moorhem, C. Lai, M. Culot, V. Rogiers, R. Cecchelli, C.C. Naus, W.H. Evans, L. Leybaert, Ca^{2+} regulation of Connexin-43 hemichannels in C6 glioma and glial cells, Cell Calcium 46 (2009) 176–187.
[72] A. Dovas, A. Yoneda, J.R. Couchman, PKCβ-dependent activation of RhoA by syndecan-4 during focal adhesion formation, J. Cell Sci. 119 (2006) 2837–2846.
[73] E.S. Oh, A. Woods, S.T. Lim, A.W. Theibert, J.R. Couchman, Syndecan-4 proteoglycan cytoplasmic domain and phosphatidylinositol 4,5-bisphosphate coordinately regulate protein kinase C activity, J. Biol. Chem. 273 (1998) 10624–10629.
[74] J.H. Luo, I.B. Weinstein, Calcium-dependent activation of protein kinase C. The role of the C2 domain in divalent cation selectivity, J. Biol. Chem. 268 (1993) 23580–23584.
[75] S. Armstrong, A. Pereverzev, S.J. Dixon, S.M. Sims, Activation of P2X7 receptors causes isoform-specific translocation of protein kinase C in osteoclasts, J. Cell Sci. 122 (2009) 136–144.
[76] W.A. Altemeier, S.Y. Schlesinger, C.A. Buell, W.C. Parks, P. Chen, Syndecan-1 controls cell migration by activating Rap1 to regulate focal adhesion disassembly, J. Cell Sci. 125 (2012) 5188–5195.
[77] J.A. Roper, R.C. Williamson, M.D. Bass, Syndecan and integrin interactomes: large complexes in small spaces, Curr. Opin. Struct. Biol. 22 (2012) 583–590.
[78] P. Schneider, Production of recombinant TRAIL and TRAIL receptor: Fc chimeric proteins, Methods Enzymol. 322 (2000) 325–345.